Nitrogen Controls on Climate Model Evapotranspiration

ROBERT E. DICKINSON,* JOSEPH A. BERRY,+ GORDON B. BONAN,# G. JAMES COLLATZ,@ CHRISTOPHER B. FIELD,+ INEZ Y. FUNG,& MICHAEL GOULDEN,** WILLIAM A. HOFFMANN,++ ROBERT B. JACKSON,## RANGA MYNENI,@@ PIERS J. SELLERS,&& AND MUHAMMAD SHAIKH*

**Georgia Institute of Technology, Atlanta, Georgia*
+Department of Plant Biology, Carnegie Institution, Stanford, California
#National Center for Atmospheric Research, Boulder, Colorado
@NASA Goddard Space Flight Center, Greenbelt, Maryland
&Center for Atmospheric Sciences, University of California, Berkeley, Berkeley, California
***Department of Earth System Science, University of California, Irvine, Irvine, California*
++Department of Botany, University of Brasilia, Brasilia, Brazil
##Department of Botany, Duke University, Durham, North Carolina
@@Department of Geography, Boston University, Boston, Massachusetts
&&NASA Johnson Space Flight Center, Houston, Texas

(Manuscript received 27 June 2000, in final form 22 February 2001)

ABSTRACT

Most evapotranspiration over land occurs through vegetation. The fraction of net radiation balanced by evapotranspiration depends on stomatal controls. Stomates transpire water for the leaf to assimilate carbon, depending on the canopy carbon demand, and on root uptake, if it is limiting. Canopy carbon demand in turn depends on the balancing between visible photon-driven and enzyme-driven steps in the leaf carbon physiology. The enzyme-driven component is here represented by a Rubisco-related nitrogen reservoir that interacts with plant–soil nitrogen cycling and other components of a climate model. Previous canopy carbon models included in GCMs have assumed either fixed leaf nitrogen, that is, prescribed photosynthetic capacities, or an optimization between leaf nitrogen and light levels so that in either case stomatal conductance varied only with light levels and temperature.

A nitrogen model is coupled to a previously derived but here modified carbon model and includes, besides the enzyme reservoir, additional plant stores for leaf structure and roots. It also includes organic and mineral reservoirs in the soil; the latter are generated, exchanged, and lost by biological fixation, deposition and fertilization, mineralization, nitrification, root uptake, denitrification, and leaching. The root nutrient uptake model is a novel and simple, but rigorous, treatment of soil transport and root physiological uptake. The other soil components are largely derived from previously published parameterizations and global budget constraints.

The feasibility of applying the derived biogeochemical cycling model to climate model calculations of evapotranspiration is demonstrated through its incorporation in the Biosphere–Atmosphere Transfer Scheme land model and a 17-yr Atmospheric Model Inter comparison Project II integration with the NCAR CCM3 GCM. The derived global budgets show land net primary production (NPP), fine root carbon, and various aspects of the nitrogen cycling are reasonably consistent with past studies. Time series for monthly statistics averaged over model grid points for the Amazon evergreen forest and lower Colorado basin demonstrate the coupled interannual variability of modeled precipitation, evapotranspiration, NPP, and canopy Rubisco enzymes.

1. Introduction

The balancing of absorbed solar energy by evapotranspiration (ET) is a major determinant of land surface temperature and other features of climate. Hence, climate models attempt to represent the mechanisms most important for determining ET and its connections to other elements of the climate system. Recently, so-called ''third generation'' land surface models (e.g., Collatz et al. 1991; Sellers et al. 1996; Bonan 1995; Foley et al. 1996; Dickinson et al. 1998) have included a treatment of photosynthesis to describe the stomatal controls on ET (e.g., Sellers et al. 1997, and in Fig. 1). Plants transpire as a by-product of their requirement for leaves to assimilate carbon. A key parameter is a leaf's capacity for photosynthesis, V_{max}, which is known to have a strong association with leaf nitrogen (N) content (e.g., Field and Mooney 1986).

Hence leaf N could be prescribed as an alternative to V_{max}. However, N does not occur in fixed amounts in any given leaf but rather responds to overall plant–soil nitrogen cycling processes. These cycling processes are

Corresponding author address: Robert Dickinson, School of Earth and Atmospheric Sciences, Georgia Institute of Technology, 221 Bobby Dodd Way, Atlanta, GA 30332-0340.
E-mail: robted@eas.gatech.edu

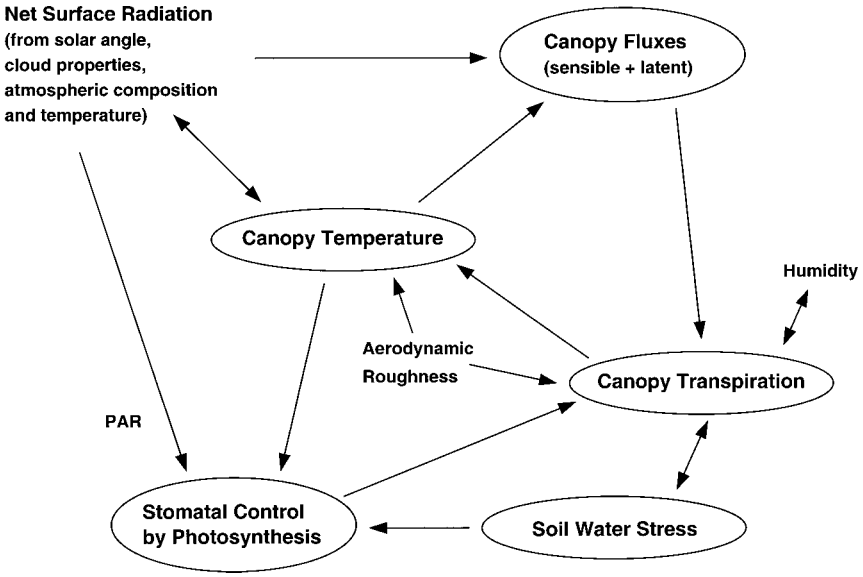

FIG. 1. Schematic of how canopy photosynthetic capacity couples to a climate model.

in turn strongly connected to various climate parameters such as temperature and precipitation. Thus, it can be argued that neither plant photosynthetic capacities nor stomatal function parameters should be specified empirically in a climate model but rather both should be jointly derived with N-cycling processes as they interact with the climate system and soil processes. That the subsequent feedbacks might be substantial are indicated by measurements reported by Seligman et al. (1983) and showing that a wheat canopy fertilized with nitrogen was 4°C cooler than one under nitrogen stress. However, dependencies of evapotranspiration on variations in nitrogen have not been previously included in climate models.

A model for leaf-level photosynthesis and transpiration is here combined with a canopy-level light and temperature model to determine canopy-average carbon fluxes as sketched in Fig. 2. Carbon assimilated by the leaves is allocated to leaves, roots, and wood by minor modifications of the rules described in Dickinson et al. (1998). However, leaf V_{max} is determined from modeled leaf nitrogen rather than being prescribed. Atmospheric inputs and land boundary conditions are provided by the overall climate model framework. The resulting model of coupled carbon–nitrogen cycling attempts to represent ''generic'' vegetation rather than the behavior of particular ecosystems, beyond the physical parameters for different land covers that are already included in the climate model and a few obvious additional parameters. The only prescribed ecosystem-connected leaf parameter is the specific leaf area (SLA = leaf area per unit mass). Many important species-specific plant processes that may be very significant for canopy radiation and carbon assimilation are thus not considered, as for example, phenology beyond that dictated by the response of leaf growth to radiation, temperature, and soil moisture.

The first treatments of vegetation in climate models such as in the Biosphere–Atmosphere Transfer Scheme (BATS) model (Dickinson et al. 1993) specified empirical relationships between leaf stomatal controls of transpiration and environmental parameters such as temperature and light levels. The more recent formulation in terms of leaf carbon assimilation (as reviewed by Sellers et al. 1997) provides an interface for calculation of carbon budgets and dependences on the concentrations of atmospheric carbon dioxide, but otherwise can be viewed as an improved version of the same model with a single basic parameter required to be specified, since a constant V_{max} is functionally equivalent to the earlier specified minimum stomatal resistances, and either set of parameters can be given as a table for the different model land covers. However, measurements of both sets of parameters have shown substantial variation even for the same plant species. In addition, climate models require not simply leaf stomatal properties, but also the surface area of the leaves. Both the leaf stomatal functioning and leaf areas that provide the plant controls on evapotranspiration adjust on timescales of weeks to seasons. Such variation could be included seasonally as tables for the land cover types represented in a given climate model. However, it is more realistic to make these dependences an interactive component of the climate model. Leaf area is determined from the modeled carbon assimilation from rules for distribution between plant components by allocation and for losses by respiration and mortality (Dickinson et al. 1998). However, variations of the stomatal functioning are controlled by variations of the Rubisco enzyme and thus by levels of leaf nitrogen. Hence, enhancing the realism of the sto-

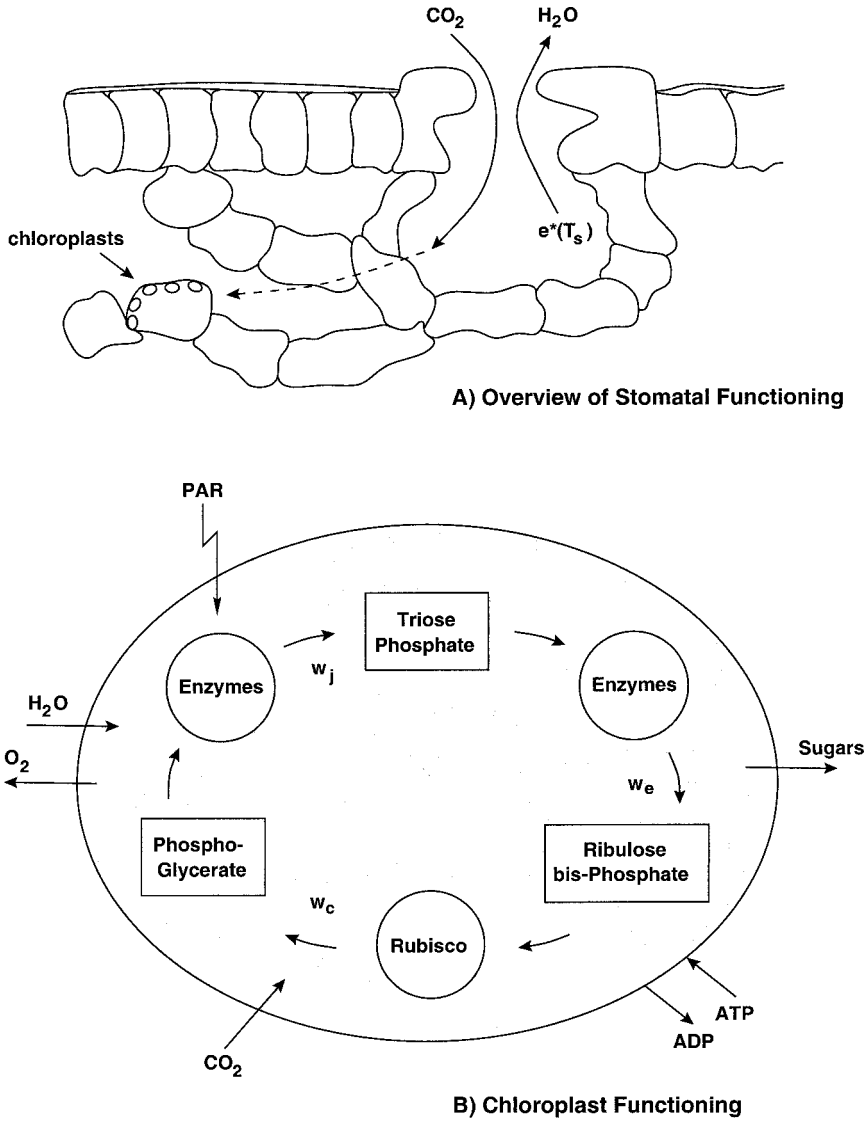

FIG. 2. The currently standard leaf-level model for climate model transpiration and carbon assimilation: (a) illustrates the transport of water and carbon dioxide through the stomatal opening, and the further diffusion of carbon dioxide through cell walls into photosynthesis sites in the chloroplast; (b) shows as a schematic blowup, the modeled (greatly abbreviated) Calvin cycle of photosynthesis. The first step, frequently rate limiting, joins CO_2 to the ribulose (5-carbon sugar) phosphate and is proportional to the concentrations of the Rubisco enzyme; the second series of steps, using photon-derived energy adds hydrogen from water, and the third series of steps, exports sugars and reconstitutes the ribulose phosphate starting point (for more details, see, e.g., Quick and Neuhaus 1997).

matal controls of evapotranspiration in a climate model requires inclusion of the sources and sinks of leaf nitrogen. This inclusion in turn requires modeling at each land grid point of the other elements of the terrestrial nitrogen cycle. Such terrestrial systems have already been studied for other purposes. The parameterizations most useful here are necessarily much simpler than would be used for a detailed process model (as reviewed for soil carbon in Moorhead et al. 1999). However, any choices made as to the level of detail to be included are not likely to be uncontroversial or to be viewed as useful for all the possible applications of such a model. The formulation of soil processes has been especially oversimplified to avoid presenting an impression that the present model is intended to be at the same level of realism as the currently most advanced soil biogeochemical models. The formulation of the underlying BATS land model precludes including the realism of vertical soil layering. The component carbon stores have been deliberately further oversimplified. The intent is

to prototype a very complex system rather than attempt a final definitive treatment.

This question as to whether or not to include nitrogen cycling and at what level of detail is somewhat analogous to the question as to the appropriate strategy for the inclusion of interactive cloud properties in climate models. Most climate models concluded several decades ago that whatever cloud properties that interact with the larger scale could in principle be calculated interactively should be so calculated rather than put in observationally. However, because there has been no agreed upon recipe to achieve a validated treatment of such properties, this problem of deriving cloud parameterizations is still being addressed by modelers. The basic reason for introducing any such new parameterization into a climate model is that it improves the realism of the model and that it makes a difference for model performance but that it does not degrade the usefulness of the model for its primary intended applications. The land components of climate models have, like cloud properties, not been amenable to rigorous model validation procedures but do undergo extensive evaluations, often through community intercomparisons between different versions of the same parameterization. Single site data has been of some but generally limited usefulness since adjusting model parameters to best match such data is of little generality for a global model intended to apply across all systems. Testing of a new parameterization by coupling to a climate model is time consuming but quite necessary. With increased complexity, model simulations often compute values outside the anticipated range of parameter space and consequently can give physically unrealistic results until the parameterizations have been made adequately robust for climate model usage. Increased complexity may also make a computation unnecessarily costly in terms of computer resources and the requirements for analysis of results. Hence, it is normally better initially to err on the side of oversimplification rather than of excess detail.

Although the controls of evapotranspiration by leaf nitrogen levels are fundamental, correctly included, they should not be expected to be highly evident in changing simulations because of the many other variable factors that are of equal or greater importance for evapotranspiration, especially those involving energy and water balances. The changes introduced are too complex to be susceptible to interpretation as differences between a control simulation without the changes and the modified model. Simple changes in relevant climatological parameters such as temperatures or runoff ratio would more likely point to inadvertent shifts in the average properties of the stomatal functioning than to the impact of the increased degrees of freedom. The primary evaluation procedures used here are to look at examples of the new model output fields, to examine their reasonableness, and to examine correlation statistics indicating the connections between the time variations of nitrogen-cycling parameters and those components of the climate model that are already recognized as important. Past literature as summarized in Sellers et al. (1997) adequately demonstrates the importance of stomatal functioning for the simulation of terrestrial climate. Our analysis has not attempted to provide further evidence for that assertion but rather to show that given the importance of the stomatal functioning for climate models, inclusion of nitrogen controls makes a quantitative difference and improves the realism of the treatment.

2. N-Cycling issues controlling canopy stomatal functioning

Establishing a model of the controls of ET by N cycling requires addressing several issues:

1) lack of a clear understanding as to what determines the allocation of N among different components of plants, including how much of leaf N goes into determining photosynthetic capacity;
2) lack of quantitative understanding of what plant feedbacks and competition with microbiota limit the uptake of N from the soil and what are the connections between growth and nutrient needs;
3) difficulties in quantitative specification of the addition and removal processes for N between the plant–soil continuum and the atmosphere–hydrosphere systems (these processes are sketched in Fig. 3).

a. Plant N allocation

Plants allocate N for various requirements such as formation of flowers and fruits. However, here it is only allocated to leaves or fine roots. The concentrations of N in fine roots may differ according to various needs, but these are not represented in our treatment. Rather, we assume roots that have a structural component with a prescribed ratio of N/C (C = Carbon) plus a labile component whose N content may vary between this prescribed ratio and zero, depending on the availability of N for photosynthesis. Likewise, different leaves build a variety of compounds that require differing amounts of N but again, the functions of these compounds are not explicitly modeled. Rather, we are guided by observations that relate leaf N to photosynthetic capacity and by the molecular basis for photosynthesis in terms of Rubisco and related compounds. Rubisco is the leaf enzyme that catalyzes the first step of C assimilation by joining CO_2 with the 5-carbon sugar, ribulose bisphosphate. It receives prominence because of its relative inefficiency so that much of it is needed (making it the most common protein in the world) and its concentration limits the rate of photosynthesis under light-saturated conditions.

An additional complexity is that many other N compounds will vary with the Rubisco content. Furthermore, different leaves will need differing amounts of N for other functions unconnected with and not varying with

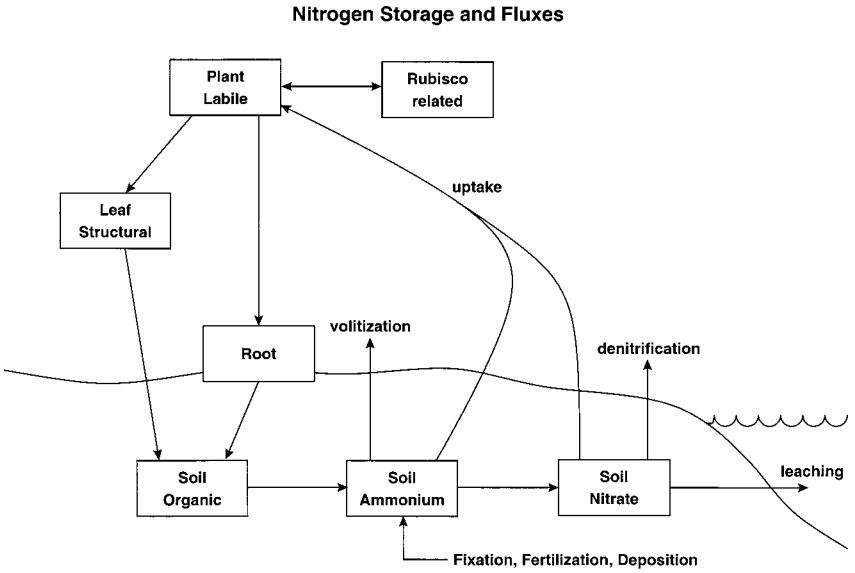

FIG. 3. Schematic of the model nitrogen reservoirs, internal fluxes between plant and soil, and external exchanges with the atmosphere and to runoff.

photosynthetic capacities (Field and Mooney 1986). The observed correlations between leaf N and photosynthetic capacity have been previously used to determine V_{max}, or maximum net assimilation, A_{max}, from N. However, different datasets suggest widely different slopes for different leaves. For example, Amthor (1994) parameterized V_{max} by inferring that a herbaceous plant would have 0.24 of its variable N in Rubisco, but deciduous trees only 0.075. The extensive data by Reich et al. (1995) on A_{max} are fitted for broadleaf deciduous trees to slopes of 5.5–6.5 micromoles s^{-1} per g of N, whereas for needle-leafed evergreens, to slopes of 0.2–1.9. As that data show, the species that have the lowest rates of photosynthesis on a per weight basis tend to have the smallest slopes. Dang et al. (1997) even report a slope of -2 (i.e., negative) for the jack pines of the Boreal Ecosystem–Atmosphere Study (BOREAS) northern study area. A smaller slope for leaves with lower values of A_{max} could be explained in terms of a correlation between nonphotosynthetic N and Rubisco. However, it is difficult to find supporting evidence at the molecular level. An alternative interpretation is adopted here; it is easily demonstrated (e.g., with a random number generator) that if the Rubisco-related variation of N is small compared to the range of random variation of the N unconnected to photosynthesis then the inferred slope of A_{max} versus N will inevitably be much lower than the actual slope.

Therefore we assume a constant slope for V_{max} versus Rubisco-related N. Leaves have a wide range of weights per unit area, or, equivalently have a wide range of SLA. The present model (Dickinson et al. 1998) prescribes SLAs for different ecosystems [in units of m^2 per kg C (kilogram Carbon)] of from 10 for evergreen needleleafs to 50 for agricultural crops. Individual species have a much wider range; Reich et al. (1998) finds SLAs in m^2 (kg C)$^{-1}$ ranging from 3 for a tree, *Juniperus monosperma,* to 108 for a forb, *Eupatorium rugesum.*

Leaves should avoid overloading with Rubisco relative to that needed to make maximum use of the light levels available for photosynthesis (Field and Mooney 1986). Midsummer noontime light levels vary little, except with clouds, so all leaves at the top of a canopy require approximately the same Rubisco per unit area to maximize their carbon assimilation. Hence, the range of photosynthetic capacity on a per area basis should be considerably less than on a weight basis. Field and Mooney, 1986, in their Figs. 1.2 and 1.3 from the ''VINE'' survey, show a greater than 2 orders of magnitude range for net photosynthesis per unit mass but a range of no more than 1 order of magnitude on a per area basis. They also show that leaves with the highest nitrogen on a mass basis also have the highest rates of photosynthesis per unit nitrogen. Across species, the thinner leaves generally have larger N/C ratio; for the above-mentioned heaviest and lightest leaves of Reich et al. (1998), the Juniper has an N/C ratio of 0.03 and the forb of 0.09. This near-constancy of N/C across a wide range of Rubisco N and C is likely a result of many of the structural requirements for N such as in membranes and cell walls scaling with the total leaf mass. The increase seen with thinner leaves is interpreted as resulting from near-constant Rubisco N on a per area basis for a given average light level, ratioed to the smaller structural carbon required.

Rubisco-related N in a leaf can vary over the range 0.1–1 g N m^{-2}, depending on the availability of N and the effects of temperature, light climatology, and respiratory requirements on determining optimum levels. The latter value would add only 0.01 to a leaf's N/C

ratio for an SLA of 10 m^2 (kg C)$^{-1}$ but as much as 0.1 for an SLA of 100. The upper limit possible for N/C is about 0.15, consistent with the data in Fig. 1.1 of Field and Mooney (1986), and what would be expected for pure protein. The SLA of the lighter leaves will vary with varying amounts of Rubisco-related N because of the varying largely carbon mass of the Rubisco enzymes. In particular, sunny leaves should become heavier than shaded leaves of the same species as often observed (e.g., Poorter and Evans 1998).

Carbon assimilation, hence ET, depends not only on Rubisco, but also on soil water and absorbed solar radiation. The absorbed solar radiation alone, as the most measurable of these, has been used by Sellers et al. (1992) to estimate canopy V_{max}, arguing that Rubisco will adjust to light levels and leaf area to available soil water and nitrogen. Such adjustments are implicit in the present formulation but occur on timescales of several weeks to many months and may not be complete. For example, the enhanced V_{max} of a fertilized over a nonfertilized field may not imply a corresponding increase in absorbed solar radiation. Many plants in semiarid regions reduce their stomatal conductance without much leaf and hence presumably without much nitrogen loss, in response to water stress.

b. Root uptake

Variations in leaf Rubisco, hence photosynthetic capacity, are likely related to variations in root uptake of N, responding either to soil scarcity or conversely, excess leaf supply. The soil supplies N to the roots in the form of nitrate, ammonium ions, and amino acids (Ourry et al. 1997). This N is delivered through transpiration-driven water flux and molecular diffusion through the pore water. Roots normally maintain a capability to acquire N at a faster rate than can be supplied by the physical transport delivery, through maintaining low internal concentrations and active ion pumps. Conversely, excess internal supplies of N can reduce root uptake to rates below that of the capacity of soil delivery processes. These reductions of N uptake at the soil–root interface depend on various mechanisms such as root ejection of bicarbonate ions generated in the reduction of nitrate ions in the leaves, and a response to the buildup of nitrogen-containing metabolites, that is, amino acids, in the phloem (Ourry et al. 1997). Plants take up N much more rapidly in daylight than in darkness and this uptake can be suppressed by large concentrations of CO_2. Either with low light or with excess CO_2, a leaf will have excess Rubisco capacity relative to that which is needed, and biochemical feedbacks should limit further Rubisco production. In addition, much of the energy required to assimilate nitrate ions, and possibly to synthesize Rubisco as well, is supplied by photosynthetic energy, which could be limited by priority given to carbon assimilation.

The idea that leaves equilibrate to some N levels for given light levels (Field 1983; Haxeltine and Prentice 1996) can be satisfied by instantaneous constraints on the fraction of photosynthate allocated to leaf respiration (Dewar et al. 1998). However, it is more consistent with our current understanding of leaf molecular processes to hypothesize that plants respond to the various signals such as amino acid buildup to limit N uptake from the soil when the Rubisco-driven component of leaf carbon assimilation has excess capacity. This response is likely mediated by buildup of nitrogen-containing compounds in photosynthate exported from the leaves and hence might be weakened by any of the other plant requirements for N that we have not attempted to include.

c. Sources and sinks

Although the annual supply of N in natural systems is largely supplied by recycling, it cannot be entirely so because of various slow loss processes. On a magnitude basis, plants must take up 10 g m^{-2} N annually from a soil mineral reservoir containing 1 g m^{-2} N and deliver this N back to the soil (e.g., Table 6). Furthermore, a 1 g m^{-2} external source of N must be balanced by a 1 g m^{-2} annual loss. These balances can be achieved if mineral N is lost from the system at a rate of 1 yr^{-1} and it is taken up by plants 10 times as fast.

The sources of N are currently about half natural and half anthropogenic. Galloway et al. (1995) have reviewed the current understanding of the global distribution of biotic and anthropogenic nitrogen fixation. Biotic fixation on continents is estimated to be in the range 90–130 Tg yr^{-1} (0.6–0.9 g m^{-2} yr^{-1} on average over land), and human activities to add additional nitrogen consisting of 20 Tg by energy production, 80 Tg by fertilizers, and 40 Tg by cultivation of nitrogen-fixing crops. A substantial fraction of the added nitrogen can be removed by harvest (Howarth et al. 1996, their Table 4). We include N losses to harvest, but do not model further conversion from the harvested material beyond lumping it with other contributions to the atmospheric deposition term.

Overall, about 30% (34 Tg yr^{-1}) of nitrogen fixed by anthropogenic activity is redeposited from the atmosphere as ammonium ions to terrestrial systems, having been lost to the atmosphere by animal wastes, volatilization of fertilizer, and biomass burning (Dentener and Crutzen 1994; Galloway et al. 1995; Bouwman et al. 1997). In addition, oxides of nitrogen are released to the atmosphere by energy generation and biomass burning, (about 21 Tg yr^{-1} deposited on land). Spatial patterns of this deposition have been generated by various atmospheric models (e.g., as discussed by Holland et al. 1997). Globally averaged over land, natural systems fix about 0.8 g N m^{-2} yr^{-1}, and receive about half that much from atmospheric deposition, whereas agricultural lands, composing about 10% of global land area, receive about 10 times as much from fertilization application and promotion of leguminous crops.

3. Formulation for carbon and nitrogen controls of stomatal functioning

a. Carbon

The carbon formulation is modified from that of Dickinson et al. (1998). It consists of three elements:

1) a simple representation of carbon reservoirs, consisting of photosynthate, leaf, wood, root, and fast and slow soil compartments; temperature dependent rates for leaf, root, and soil respiration; and rules for death, harvest, or fire losses from the live compartments;
2) some rules for allocation of assimilated carbon between the photosynthate, leaf, root, and wood stores;
3) a description of leaf carbon assimilation for C-3 plants based on Farquhar et al. (1980).

1) Carbon reservoirs and allocation

Equations from appendix B in Dickinson et al. (1998), for carbon stores, are supplemented with a photosynthate reservoir. This reservoir serves two purposes:

1) it provides a rapid leaf growth at the beginning of a growing season, and
2) it provides a more realistic energy source for respiration, especially at times of negative carbon accumulation.

Without this term, leaf area is lost whenever net leaf carbon assimilation is negative because of dominance by respiration, and an unrealistic day–night fluctuation in leaf area index (LAI) occurs. The photosynthate reservoir also prevents long-term loss of LAI to respiration when there is an excess of Rubisco-related enzymes.

Total leaf carbon consists of a structural pool, related to LAI by a prescribed SLA, the photosynthate pool, which is normally nearly an order of magnitude smaller, and that incorporated in Rubisco-related structures, which will normally be even smaller than that of the pool of photosynthate, and is neglected unless the photosynthate declines to zero. If that happens, further respiratory costs are met by shrinking the Rubisco-related nitrogen pool, assuming 10 g C are provided per g of N lost. The resulting carbon fluxes are neglected as consistent with neglect of a carbon pool accumulated with Rubisco. Such a respiratory decay of Rubisco may be an essential feedback for leaves to reduce their photosynthetic capacities to those needed for given light levels.

The equation for the photosynthate reserve C_p, representing labile sugars and stored starches that can convert back to sugars, is (see appendix for the definition of variables used in all equations).

$$\frac{dC_p}{dt} = f_p \times X_c - k_p \times F \times C_p - \text{all respiration terms}, \quad (1)$$

where the transfer of photosynthate to leaf structure scales with a maximum rate k_p and is modulated by the factor

$$F = (1 - f_p)\exp(-\text{LAI}) \times 1/(1 + S_{\text{cd}}), \quad (2)$$

a factor that approaches 1 for small LAI and nonstressed growing conditions, but becomes very small for large stress or large LAI. The fraction of assimilated carbon X_c that is allocated to C_p is given by

$$f_p = \frac{\{[1 - \exp(-\text{LAI})]\exp(-C_p/C_{\text{po}}) + S_{\text{cd}}\}}{(1 + S_{\text{cd}})}, \quad (3)$$

where the dependence on LAI allows the allocation to go directly to the leaves in the limit of small LAI and the assumption $C_{\text{po}} = 100\ \text{g m}^{-2}$ allows C_p to equilibrate for full canopy at about 50 g m^{-2}, when about half of carbon assimilation is needed to pay respiratory costs. Although a single value is used here, the appropriate value for C_{po} could vary widely between different kinds of vegetation depending on, among other things, the biomass of a plant. The term S_{cd} is the sum of the cold and drought stress terms defined by Eqs. (7) and (8) in Dickinson et al. (1998).

Previous allocation to leaf, root, and wood are multiplied by $(1 - f_p)$, and the previous carbon equations for these reservoirs no longer include any respiration terms. Daytime leaf respiration is accounted for in carbon assimilation, that is, Eq. (18a), and so not included in Eq. (1).

The photosynthate reserve, consisting of whatever forms of carbon stores are available for oxidation in the mitochondria to generate energy needed by the plant, provides respiration costs but otherwise has no control on respiration unless it vanishes. Leaf respiration is reformulated in the next section [Eqs. (14)–(16)]. We have added an ion uptake cost of 1.5 g C per g N assimilated and a fixation cost of 10 g C per g N fixed (e.g., Gutschick 1981; Eissenstat and Yanai 1997; Serraj et al. 1999). Leaf carbon is increased by direct allocation or by transfer from the photosynthate pool and is lost by stress death, turnover, and harvest, as follows:

$$\frac{dC_l}{dt} = (1 - f_p) \times S_n \times f_{\text{cl}} \times X_c + k_p \times F \times C_p - (k_s S_{\text{cd}} + k_{\text{lt}} + k_h)C_l, \quad (4)$$

where k_s is a scaling rate for leaf drought or cold stress and where S_n is nitrogen stress factor to be defined later that converts a fraction $1 - S_n$ of leaf to root allocation. The term k_{lt} is the leaf turnover rate for senescence and herbivory, introduced in Dickinson et al. (1998) and modified as described in the next section [Eq. (18b)], and the rate k_h is a leaf removal rate by harvest, prescribed as nonzero for agricultural systems.

2) Assimilation

The assimilation parameterization of Dickinson et al. (1998) borrowed heavily from earlier studies by Collatz

et al. (1991), Sellers et al. (1996), Bonan (1995), and Foley et al. (1996) among others and has been further modified for the present paper. Parameters have been assessed from recent physiological studies. However, the only substantial modification to the earlier formulations has been the inclusion of resistance to leaf internal transport of carbon (e.g., Evans and von Caemmerer 1996). This term is included to provide greater physiological distinction between leaves of different thickness.

The minimum of three rates determines leaf carbon assimilation. These are the light-driven rate w_j, and the Rubisco catalysis and photosynthate export rates, w_c and w_e, respectively. The light-driven rate is assumed to be linear in absorbed visible light, as most appropriate for low-light levels, and so the only form of light saturation included is that implied by the Rubisco-controlled rates. Hence,

$$w_j = w_{j0} \times \text{PAR}, \tag{5}$$

where PAR is photosynthetic radiation in W m^{-2}. Light use efficiency has been reviewed by Foyer and Harbinson (1997), who argue that on a quantum basis, it should be less than 12.5%. Long et al. (1993) report on an absorbed quanta basis, that the measured efficiency varies little between species, and is about 9%. Hence, we express w_{j0} in μmoles J^{-1} as

$$w_{j0} = 0.425 \times \frac{[1 - 0.1\lambda_c \times f(T)]}{[1 + 0.2\lambda_c \times f(T)]}, \tag{6}$$

where $f(T)$ is the single exponential temperature dependence, adopted for all model rates involving the speedup of enzyme activity with temperature,

$$f(T) = \exp[0.08(T - 298)], \tag{7}$$

and λ_c is the ratio of CO_2 of a prescribed reference value to that at the Rubisco site, calculated by balancing carbon fluxes with carbon assimilation.

The rate at which Rubisco can assimilate carbon w_c is written:

$$w_c = V_m \times \frac{[1 - 0.1\lambda_c \times f(T)]}{[1 + 2\lambda_c \times f(T)]}, \tag{8}$$

where V_m is the maximum assimilation rate possible in the limit of large CO_2 concentrations, taken to be

$$V_m = b \times \hat{N}_{\text{rub}} \times f(T) \div [1 + 0.04 f(T)^3], \tag{9}$$

where $b = 200$ μmoles g^{-1} s^{-1} is the assumed slope for correlation of carbon assimilation with Rubisco-related nitrogen, and $\hat{N}_{\text{rub}}$ is the Rubisco-related leaf nitrogen in units of g m^{-2}, specified as a profile for calculation of V_m, but as an average value for leaf respiration [Eqs. (15)–(17)]. The denominator in Eq. (9) gives the high temperature loss of capacity due to thermal damage. The factor of 2 in the denominator of Eq. (8) represents both a CO_2 limitation and the competition with oxygen for the first step of the Calvin cycle. The subtracted term in the numerator represents the photorespiration losses for a C3 plant. The physiological parameters used are those given in Poorter and Evans (1998) and differ somewhat from the ''Collatz–Bonan'' values we previously adopted. Because these parameters are rather uncertain, at most one decimal place of accuracy is possible. The λ_c term will typically be about 2.

The last term needed w_e, sometimes referred to as the ''export-limited rate'' represents the rate at which triphosphate can be utilized, and so metabolized sugars exported and the initial ribulose reconstituted. It is assumed to be the same as used by Collatz et al. (1991), and Bonan (1995):

$$w_e = 0.5\ V_m. \tag{10}$$

The numerical factor is known to lie between 1/3 and 1/2. Wullschleger (1993) reviews a wide range of measurements for V_m and triphosphate ''utilization'' (TPU), giving average values of V_m of 75 μmoles m^{-2} s^{-1} for annuals, 44 μmoles m^{-2} s^{-1} for perennials, and an average triphosphate utilization of 10.1 μmoles m^{-2} s^{-1}. Hence, simply averaging the annual and perennial rates and taking w_e as $3 \times$ TPU gives $w_e \approx 0.5\ V_m$. Foley et al. (1996) argue for a somewhat smaller value, apparently based on a different averaging approach with the same data. As evident from Eqs. (7)–(8), this term should become rate limiting, when T drops below 5°–10°C. A smaller value would raise the temperature of switchover by a few degrees.

The numerical constants in Eqs. (6) and (8) were determined for a reference concentration of 360 ppmv, appropriate to current global-average concentrations. The internal concentrations will scale with external concentrations so that other external concentrations can be assumed by multiplying λ_c by 360 and dividing it by the external carbon dioxide concentration in ppmv. Limited observations (as reviewed by Poorter and Evans 1998) suggest leaves commonly have about a 30% drop in CO_2 from leaf cavity concentrations to the photosynthesis site, independent of assimilation rates, which would only be possible if leaf internal resistances over this path are inversely proportional to assimilation rates. Thicker leaves usually have lower assimilation rates on a per mass basis and often on a per area basis. Variation in SLA is primarily due to differences in leaf thickness. It is plausible that internal resistances should scale with leaf thickness (Evans and von Caemmerer 1996). Hence, we assume a leaf internal resistance proportional to leaf thickness. Leaves acting to optimize between light and Rubisco limitations could simply add more Rubisco to compensate for an internal resistance that lowers CO_2 at the Rubisco site. However, this cannot be done without an additional respiratory cost (e.g., Dewar et al. 1998; Haxeltine and Prentice 1996), and further stress on limited supplies of nitrogen. Hence, assimilations per unit area will tend to be less for smaller SLA. Besides the effects of internal resistances, leaves for different life forms are distinguished by the dependence of their

turnover rates on leaf weight and differing thresholds for cold stress.

b. Nitrogen

1) Plant nitrogen pools

The leaf structural and root pools are determined from leaf structural and root carbon as

$$N_{\rm ls} = r_{\rm ncl} \times (1 - f_n) \times C_l \quad \text{and} \tag{11}$$

$$N_r = r_{\rm ncr} \times (1 - f_n) \times C_r, \tag{12}$$

where $r_{\rm ncl} = 0.03$ and $r_{\rm ncr} = 0.024$ are nitrogen to carbon ratios for leaf structure (inferred from Reich et al. 1998) and for roots (Gordon and Jackson 2000), whereas f_n is the fraction of the leaf structural and root nitrogen that has been moved to the $N_{\rm rub}$ pool because of shortage. We assume

$$f_n = 0.2 \exp(-2 \times N_{\rm rub}/\sigma_f) \tag{13a}$$

as estimated from some limited N-stress data of Chapin (1991). This term, multiplied by the leaf structural and root N, gives the labile N. In other words, we assume up to 20% of the leaf structural and root nitrogen is labile and can be moved to the Rubisco-related pool in the limit of extreme deprivation whereas under unstressed conditions of canopy $N_{\rm rub}$ of about 1 g m^{-2}, the f_n term is at most a few percent. It may typically be about 0.04 giving N/C ratios of 0.023 (Gordon and Jackson 2000).

Total leaf nitrogen N_l is obtained from the difference between total plant nitrogen N_p and root nitrogen N_r,

$$N_l = N_p - N_r. \tag{13b}$$

In principal, the term $N_{\rm rub}$ is in turn obtained by subtracting leaf structural $N_{\rm ls}$ from the total leaf pool N_l, that is, $N_{\rm rub} = N_l - N_{\rm ls}$. However, with direct use of this difference, leaves with small LAI after previous defoliation are unable to achieve a positive carbon uptake. The N that was previously retained by translocation from removed leaves is then almost all interpreted as Rubisco N, whose consequent respiration exceeds any possible C gain by the leaf. Presumably, most such N is not stored as proteins but in some form with little or no respiratory cost. Hence, we assume

$$N_{\rm rub} = [N_l - (1 - f_n) r_{\rm ncl} C_l](1 - f_n) r_{\rm ncl} C_l / N_l]. \tag{14}$$

This expression defines $N_{\rm rub}$ as the difference between the total leaf nitrogen and the minimum structural nitrogen at low Rubisco, multiplied by the ratio of minimum leaf structural nitrogen to total leaf nitrogen. Hence, when the total leaf nitrogen is not much larger than that needed to supply the minimum structural requirement this expression puts all the nonstructural leaf nitrogen into Rubisco; but when total leaf nitrogen becomes much larger than that needed for leaf structure, the nitrogen put into Rubisco will not exceed that put into structure.

Although most carbon models in the past have based their maintenance respiration costs on carbon, data for such a correlation is widely scattered. Respiration is much more tightly correlated with nitrogen (e.g., Reich et al. 1998; Preigitzer et al. 1998), consistent with its connection to repairs of fragile enzymes. To the extent that the leaf enzyme content is proportional to Rubisco, leaf respiration may vary with Rubisco content, hence V_m, as used in our earlier version, and by other authors, following Farquhar et al. (1980). However, daytime leaf respiration per unit leaf area R_d can be considerably less than nighttime respiration, R_n. Poorter and Evans (1998) find daytime considerably less than nighttime respiration, R_n. Poorter and Evans (1998) find daytime values on a per leaf mass basis in the range 20–40 nanomoles CO_2 g^{-1} s^{-1} whereas the survey of nighttime values by Reich et al. (1998) find values for leaves with N values comparable to those of Poorter and Evans as large as 50–60 in the same units. Further, the data of Reich et al. (1998) indicate a nonlinear dependence of nighttime respiration on leaf N such that respiration is twice as much per g N at high N than it is at low N. Evidently, Rubisco N can cost up to twice as much in respiration at night as structural N costs but daytime respiration R_d may consist mostly of the respiration from the structural N. Hence, we assume for daytime leaf respiration rates (units of μmoles m^{-2} s^{-1}):

$$R_d = 0.4 f(T) \hat{N}_{\rm ls}, \tag{15}$$

whereas at night, Rubisco-related respiration is included:

$$R_n = R_d + R_r, \tag{16}$$

where

$$R_r = 0.8 f(T) \hat{N}_{\rm rub}. \tag{17}$$

The factors of 0.4 and 0.8 are chosen to be consistent with the data of Reich et al. (1998). The $\hat{}$ symbol here denotes an average leaf value in g m^{-2} obtained from the canopy nitrogen values by division by $\sigma_f \times$ LAI. Rubisco degradation rates appear to vary somewhat between species but with no noticeable difference between C-3 and C-4 plants (Esquível et al. 1998).

The Rubisco-related respiration cannot cease during the day, but it could plausibly obtain its energy requirements from photosynthesis. Hence, we assume leaf level net photosynthesis to be given by

$$A_n = \min(w_j - R_r, w_c, w_e) - R_d. \tag{18a}$$

Brief periods generally near sunrise and sunset when this term may become negative are neglected by setting any such negative values to zero. What other plant metabolic requirements are met by light-derived energy is, in general poorly known, and not accounted for here. The use of light energy for the reduction of nitrate ions in the leaves varies widely between plants (e.g., Gutschick 1981). Ecosystem nighttime leaf respiration is

TABLE 1. Loss rate coefficients in s^{-1} and inverse as implied timescales. Losses are linear in the appropriate reservoir unless other factors are indicated.

	Symbol	Rate s^{-1}	Timescale
Leaf turnover[a]	k_{lt0}	$3. \times 10^{-8}$	386 days
Leaf harvest[b]	k_h	$6. \times 10^{-8}$	193 days
Root turnover[c]	k_{rt}	$4. \times 10^{-8}$	232 days (at 298 K)
Root harvest[b]	k_{hr}	$3. \times 10^{-8}$	386 days
Wood harvet[d]	k_{hw}	$1. \times 10^{-9}$	32 yr
Maximum N uptake from mineral reservoir	k_{m0}	$5. \times 10^{-6}$	56 h
Maximum nitrification rate	k_{ni0}	$1. \times 10^{-6}$	11.6 days (at 298 K)
Maximum denitrification rate	k_{dn0}	2.5×10^{-6}	4.6 days (at 298 K)
Maximum rate of photosynthate transfer from pool to leaf	k_p	$5. \times 10^{-6}$	56 h
Leaf stress scaling rate	k_s	$2. \times 10^{-7}$	
Ammonium ion volatilization rate	k_v	$1. \times 10^{-9}$	32 yr
Soil respiration coefficient	R_{s0}	$4. \times 10^{-8}$	289 days (at 298 K)
Leaf maintenance respiration coefficient[e] (doubled for Rubisco related N)	R_{l0}	$5. \times 10^{-6}$	77 days (at 298 K)
Root maintenance respiration (per g N)	R_{r0}	$4. \times 10^{-6}$	100 days (at 298 K)
Wood maintenance respiration coefficient per g C (no symbol used)		$5. \times 10^{-10}$	63 yr (at 298 K)

[a] Multiplied by an O(1) term increasing with SLA and Rubisco-related nitrogen.
[b] Only applied to agriculture land use.
[c] Root turnover includes the temperature dependence, sqrt [$f(T)$].
[d] Only for forest types.
[e] Respiration proportional to N reservoirs and $F(T)$, but timescales refer to C. Not included here are construction, root ion uptake and fixation carbon costs.

obtained from Eq. (16) by use of N_{ls} and N_{rub} in Eqs. (15)–(17).

To allow for the shorter lifetimes of thinner leaves and the greater attractiveness of high-nitrogen leaves to herbivores, leaf turnover per canopy carbon mass has been modified to

$$k_{lt} + k_{lt0} \times [0.3 + 0.010 \times (0.5N_{rub} + 1 \text{ g m}^{-2}) \times L_c], \quad (18b)$$

where L_c is the specific leaf area in $m^2\ g^{-1}$, and k_{lt0} is a prescribed rate (Table 1).

2) CYCLING EQUATIONS

The nitrogen cycling consists of external sources and sinks, and three pools of nitrogen per unit land area: (i) plant nitrogen N_p; (ii) soil and litter organic nitrogen N_s; and (iii) soil mineral nitrogen N_m. Vegetation gains N by root uptake of mineral nitrogen N_m at a rate k_m and loses N by death of plant parts, that is,

$$\frac{dN_p}{dt} = k_m N_m - \Delta N_s, \quad (19)$$

where ΔN_s is the loss of plant nitrogen to litter and soil,

$$\Delta N_s = k_{rt} N_r + \gamma_r (k_s \times S_{cd} + k_{lt}) \times (N_{ls} + N_{rub}), \quad (20)$$

where $1 - \gamma_r$ is a retranslocation coefficient for leaves (i.e., fraction of recapture into the plant when the leaf dies), assumed to be 0.5 following Aber et al. (1997), k_{rt} and k_{lt} are the root and leaf turnover rates, and S_{cd} the sum of terms for the cold and drought mortality [Dickinson et al. 1998; Eqs. (7) and (8)]. Retranslocation of nutrients in roots is neglected here, as it appears to be much smaller than in leaves (see Gordon and Jackson 2000, and references therein).

The soil and root processes of ion uptake are nondimensionalized so that their timescales are clearly evident, that is, nitrate and ammonium ions are assumed to be taken up by plants according to

$$k_m = k_{m0} \times \min(\lambda_r, \lambda_t) \quad (21)$$

$k_{m0} = 5.10^{-6}\ s^{-1}$ is a base rate, and where, λ_r, λ_t are nondimensional rates of ion uptake by respectively, high and low affinity transport at the root interface, and by physical transport by ion diffusion and bulk flow (e.g., Jungk and Claassen 1997). The rate λ_r, as measured, differs for each ion and each type of vegetation. Some species preferentially take up ammonium and some nitrate ions. These uptake rates have not been measured for most natural species. In addition, the transport through the root interface depends on ion concentrations at the root interface, which can only be determined precisely with a 3D model of ion concentrations in the root zone. However, when physical transport is not limiting, the concentrations at the root will not be significantly lower than average soil values. In addition, the variability between species is at least as large as the differences between active ion uptake of ammonium versus nitrate. Hence, as a consistent simplification, we assume the same form for all species and both ions expressed as

$$\lambda_r = h_p\left(\frac{C_r}{C_{\rm ro}}\right) \times \left(\frac{r_{\rm ref}}{r_r}\right) \times \frac{(I_{\rm max}/N_m + K_1)}{(1 + K_m/N_m)}, \quad (22a)$$

where $r_{\rm ref} = 0.5$ mm and r_r is the characteristic root radius assumed here to be $r_{\rm ref}$, and where C_r and $C_{\rm ro}$ are the root carbon and a reference value, $C_{\rm ro} = 250$ g m^{-2}, N_m is either the concentration of ammonium ions NH_4^+ or of nitrate ions NO_3^- normalized by 1.0 g m^{-2}, and K_m and $I_{\rm max}$ are nondimensional root physiological parameters, $I_{\rm max} = 1.0$, and $K_m = 0.4$, $K_1 = 0.2$, (inferred from the measurements by Kronzucker et al. 1996 for spruce uptake of NH_4^+), and h_p represents reduction of root uptake by light-limited canopy, and is assumed to have the form

$$h_p = \{1 - \exp[-\max(0.01, w_j/w_c)]\}, \quad (22b)$$

where w_j and w_c are the rates defined by Eqs. (5) and (8), such that root physiological uptake is reduced at low light or equivalently, high Rubisco, to 1% of its high light value.

The transport term λ_t is defined separately for each ion to be of the form

$$\lambda_t = \lambda_d + \lambda_{\rm et}, \quad (22c)$$

where for a soluble ion, such as nitrate, the diffusion transport rate, λ_d is assumed to be

$$\lambda_d = 0.4s \times (C_r/C_{\rm ro}) \times (D_i/D_{\rm ref}) \times (r_{\rm ref}/r_r)^2, \quad (22d)$$

where D_i = ion diffusion coefficient in saturated soil here assumed to be $D_{\rm ref}$ (which is $D_{\rm ref} = 2 \times 10^{-6}$ cm^2 s^{-1}), s is the root zone soil moisture in BATS, normalized by wet soil values (porosity), so that it ranges from 0 to 1 with smaller roots needing less mass for the same diffusion uptake. The product of root carbon and inverse radius squared is proportional to root length. The ET-driven bulk flow rate is given by

$$\lambda_{\rm ET} = 0.2\ {\rm ET}/(s \times {\rm ET}_0), \quad (22e)$$

where ET_0 is a reference value for ET; here $ET_0 = 17$ mm day^{-1} and generally it should be scaled inversely with depth of rooting zone, as shallower roots extract more water per unit soil volume. Because ammonium is less soluble, it is importantly affected by sorption by soil particles (Barber 1984), crudely allowed for here by multiplying the ammonium concentrations by 0.3. This diffusion term assumes adequate precipitation and/or new root growth to carry nutrients supplied by mineralization to the vicinity of the roots. For ''field capacity'' values of $s \sim 0.5$, the dimensional ET and diffusion uptake rates are both about 10 days. The shift to a relatively greater contribution from the ET term as the soil becomes drier may be reduced by an accompanying reduction in ET.

Changes of the soil and litter organic nitrogen, N_s are determined from

$$\frac{dN_s}{dt} = \Delta N_s - \Delta N_m, \quad (23)$$

where ΔN_s is defined by Eq. (20), and ΔN_m is the conversion to soil mineral nitrogen, given by

$$\Delta N_m = R_{\rm s0} \times I_{\rm mob} \times N_s, \quad (24)$$

where $R_{\rm s0}$ is the soil fast carbon pool respiration rate coefficient (Table 1) and $I_{\rm mob}$ reduces mineralization of N through the immobilization by bacteria for low ratios of N_s/C_s, that is, the N_s is largely recaptured by bacteria when N_s is less than 0.05 of C_s. This effect is parameterized by

$$I_{\rm mob} = \exp(-0.05\ C_s/N_s). \quad (25)$$

Finally, ammonium and nitrate ions are determined from

$$\frac{d{\rm NH}_4^+}{dt} = S_e + \Delta N_m - (k_m + k_v + k_{\rm ni}){\rm NH}_4^+, \quad (26)$$

$$\frac{d{\rm NO}_3^-}{dt} = k_{\rm ni}{\rm NH}_4^+ - (k_m + k_{\rm dni} + k_{\rm ro}){\rm NO}_3^-, \quad (27)$$

where S_e is an external source including biological fixation, deposition, and fertilization given by Eq. (32), and ΔN_m is from Eq. (24) and the rate coefficient for plant uptake, k_m from Eqs. (21)–(22). Biological fixation, most fertilizer, and the bulk of atmospheric deposition are ammonium ion, so we have simplified by assuming all sources are this term. Equations (26)–(27) require $k_{\rm ni}$ for nitrification, $k_{\rm dni}$ for denitrification, k_v for ammonia volatilization, and $k_{\rm ro}$ for surface and subsurface (i.e., leaching) runoff removal (all given in Table 1). The partitioning of mineral nitrogen into ammonium and nitrate ions is important for the parameterization of nitrogen fixation and various removal processes. A simpler approach would be to lump together ammonium and nitrate ions and impose on them a constant denitrification rate (e.g., Potter et al. 1996 used 2% per month). However, runoff and denitrification removal rates vary widely depending on the nitrate fraction present and soil wetness.

At optimum conditions, nitrification and denitrification can respectively convert ammonium to nitrate and nitrate to gaseous nitrogen on a timescale of a week. However conditions are far from optimum for one or the other rate because nitrification requires aerobic conditions whereas denitrification anaerobic (i.e., wet conditions). Both can operate simultaneously at different sites that have different oxygen levels resulting from soil heterogeneity. Because oxygen is removed primarily by root and soil respiration, changes of these in response to soil temperature variation can provide feedback to denitrification (Smith 1997). However, here we only relate implicitly soil oxygen levels to soil water levels, by assuming the latter controls the rates of denitrification and nitrification. Denitrification may occur mostly over short periods during and after precipitation, as illustrated by the modeling results of Li et al. (1992), and will be most pronounced in poorly drained soils. We have included the dependences on soil moisture by simple fitting to figures in Parton et al. (1996) using

$$k_{\rm ni} = k_{\rm ni0} \times f(T_{\rm rz}) \times \frac{s(1-s)}{(0.25 + 1/{\rm NH}_4^+)}, \quad (28)$$

$$k_{\rm dn} = k_{\rm dno} \times f(T_{\rm rz}) \times s^B, \quad (29)$$

where $T_{\rm rz}$ is the rooting zone soil temperature, $f(T_{\rm rz})$ is given by Eq. (7), and B is the Clapp–Hornberger parameter, such that Eq. (29) scales with the inverse of the soil water potential.

The dependence of nitrification on soil ammonium ions at low levels is not readily seen in observations (e.g., as discussed by Parton et al. 1996, and possibly explained in terms of heterogeneity by Davidson and Hackler 1994), but its rate appears to be proportional to soil mineralization. The latter dependence is inevitable whatever the rate in the absence of roots, but may not hold in the presence of competition by plant uptake. Equation (28) hypothesizes that at low NH_4^+ the rate becomes small and proportional to NH_4^+. Although the denominator of Eq. (28) is speculative in detail, some such slowing of nitrification at low ammonium levels may be needed in natural systems to reduce nitrogen losses to maintain observed levels of soil nitrogen.

We have included only a slow ammonia volatilization term from natural systems taking $k_v = 10^{-9}$ s^{-1}. Dentener and Crutzen (1994) model this term as a stomatal leakage, neglecting soil contributions. Bouwman et al. (1997) review this and the larger agricultural losses to ammonia emission. The net effects of the latter are assumed to be lumped with the prescription of an agricultural net source term.

Runoff loss rate is estimated for nitrate ions from

$$k_{\rm ro} = R_{\rm off}/W_0, \quad (30)$$

where $R_{\rm off}$ is the runoff in units of mm s^{-1}, and $W_0 =$ 200 mm is an assumed average soil water store. The amount of nitrate ions leached from a field varies strongly with soil texture and cover (e.g., Fig. 6 of Howarth et al. 1996), with runoff from a sandy cropland having an order of magnitude more nitrate than that from a loamy or clay pasture. Runoff loss of ammonium ions is neglected.

Detailed data on fertilizer production and consumption could be used to disaggregate the anthropogenic component by geography and season (e.g., Matthews 1994), but the present treatment simply assumes an average anthropogenic source term for the BATS dryland and irrigated agricultural grid squares, taking for these

$$S_{\rm fert} = 2.5 \times 10^{-7} \text{ g m}^{-2} \text{ s}^{-1}. \quad (31)$$

Natural systems are assumed to be fertilized by microbiological fixation, with an assumed supply (at 298 K and low-nitrate concentrations) of $S_{\rm bf} = 1. \times 10^{-7}$ g m^{-2} s^{-1}, and to a lesser extent, by a constant rate wet and dry deposition from the atmosphere of $S_{\rm wd} = 1.5 \times 10^{-8}$ g m^{-2} s^{-1},

$$S_e({\rm natural}) = [S_{\rm wd} + S_{\rm bf}\sigma_f \times (1 - f_p) \times f(T) \times \exp(-\beta_f \times {\rm NO}_3^-)]. \quad (32)$$

The nitrogen fixation varies with fractional vegetation, with the standard enzyme temperature dependence, Eq. (7), with the fraction of assimilated carbon not put into the photosynthate pool, and with a simple negative feedback response to excess soil nitrate (e.g., Vinther 1998) with $\beta_f = 0.5$. Fixation ceases during periods of drought (Sanhueza and Crutzen 1998; Serraj et al. 1999), when the photosynthate carbon reservoir is unable to provide the energy cost. Loss from biomass burning (e.g., Sanhueza and Crutzen 1998; McNaughton et al. 1998) is neglected.

4. Climate simulations with nitrogen coupling

The climate model simulation is carried out, using a version of the National Center for Atmospheric Research (NCAR) Community Climate Model version 3 (CCM3) (Kiehl et al. 1998) that has an improved treatment of orography to suppress spectral ringing and the BATS land model to which the present treatment has been appended. Ocean temperatures are prescribed as provided by the Atmospheric Modeling Intercomparison Project (AMIP2) project. The model is integrated over a 17-yr period. The initial mineral N stores adjust rapidly to the balance or imbalance between sources and gain and loss of organic and of plant N. However, the overall system can require decades or longer to reach equilibration between the internal stores and externally prescribed sources and sinks.

Numerous earlier integrations overall or a fraction of this period were made to identify and fix model shortcomings and help spin up the slower model adjustments (such as high-latitude carbon reservoirs). Since the carbon and nitrogen cycling have been iterated to a steady state outside of high latitudes through the repeated cycling through the 17 yr of AMIP forcing, details of the initialization are somewhat irrelevant. However, they could be very important for use of any such model to match observational histories for a particular time period. Since the parameterizations link the slower N stores to carbon stores, they were not be initialized independently. Rather we assumed that $N_s = 0.05\ C_s$, and that $N_p = 0.03\ C_l + 0.024\ C_r + 1$ g m^{-2}.

The climate model calculates absorbed PAR and total radiation at the surface by attenuation of that incident at the top of the atmosphere by the gaseous and particulate composition of the atmosphere. It calculates precipitation from the atmospheric hydrological cycle and this provides soil moisture. The root and soil moisture distributions determine a maximum rate of transpiration (Dickinson et al. 1993). If the transpiration determined by carbon assimilation exceeds this demand, stomatal conductance is reduced iteratively to match the demand to the supply of soil water. This stomatal closure correspondingly reduces the carbon assimilation.

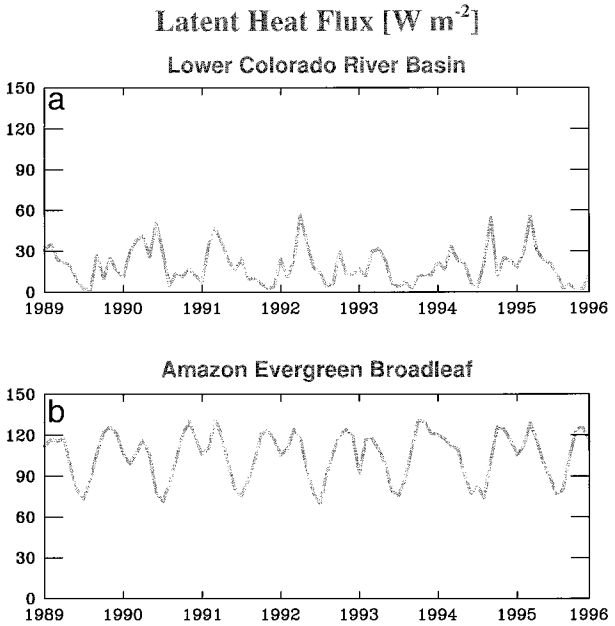

FIG. 4. Examples of monthly averaged evapotranspiration in energy units W m^{-2} (1 W m^{-2} is approximately equivalent to 1 mm $month^{-1}$) averaged over selected model grid cells from the beginning of 1989 to end of 1995: (a) lower Colorado basin points, and (b) Amazon evergreen broadleaf points.

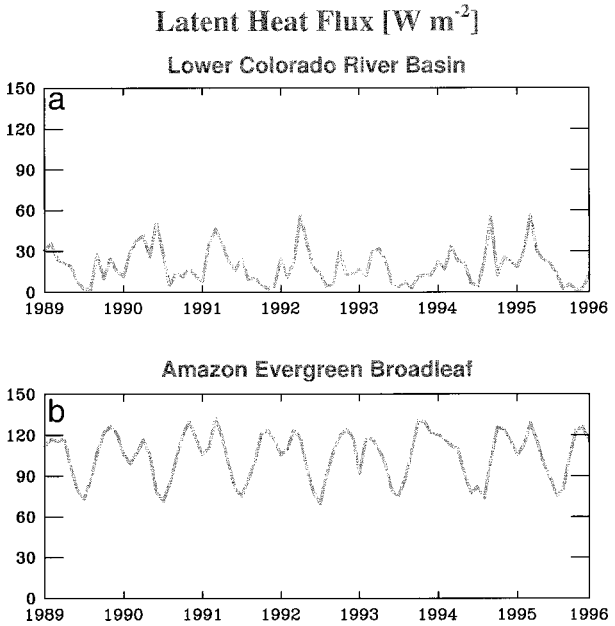

FIG. 5. Same as Fig. 4 but showing the net plant carbon net primary production (NPP) (assimilation) in g C day^{-1}.

The model puts out hundreds of standard climatological parameters. Many of these have been adequately considered elsewhere, and any changes in them from the present formulation are likely to be difficult to determine. Hence, the paper examines the climatological appearance of the evapotranspiration, carbon assimilation, and Rubisco nitrogen. All the new variables were averaged monthly over the BATS land cover types, as well as over specific geographical regions and hemispheres of the globe.

From the several dozen averaging regions, we have selected two for discussion, that is, an average over those points representing the lower Colorado basin (6 points) and an average over the Amazon broadleaf evergreen model grid squares (69 points). Figures 4 and 5 compare evapotranspiration and carbon net primary production (NPP) (assimilation) for these two regions over the last 7 years of the simulation. Both regions and both fields show pronounced seasonal cycles and substantial interannual variability. The lower Colorado basin shows summer dryness and large variations in the peak winter precipitation, as seen in the evapotranspiration. The modeled dry season reductions in evapotranspiration and net carbon assimilations are exaggerated, at least over parts of the Amazon because of greater seasonality of precipitation and shallower rooting depths in the model than observed. The Amazon tends to have reduced precipitation during El Niño years, as also seen by reductions in evapotranspiration and to a lesser extent, carbon assimilations. The Southern Hemisphere, showing a dry season from June to October, dominates the Amazon averages. Figure 6 shows the corresponding time series for the Rubisco-related nitrogen pool. Interannual variations of individual months over the 17 yr of the 3 plotted time series are highly correlated. The monthly values of Rubisco nitrogen for each point over the Amazon correlate with the latent heat flux at values ranging from 0.93 during the wet season to as much as 0.99 during the dry half of the year.

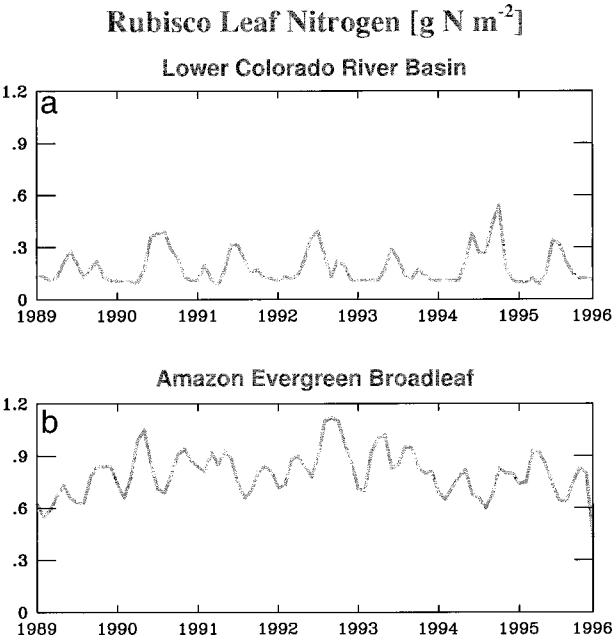

FIG. 6. Same as Fig. 4 but showing the Rubisco-related leaf nitrogen in g N m^{-2}.

TABLE 2. Prescribed source terms for fixed N in g m^{-2} s^{-1} with g m^{-2} yr^{-1} in parentheses.

	Term	
Maximum natural fixation at 298 K	S_{bf}	$4. \times 10^{-7}$ (19.7)
Wet and dry deposition	S_{wd}	1.5×10^{-8} (0.47)
Fertilizer (only agricultural lands)	S_{fert}	2.35×10^{-7} (7.41)

The model parameters related to the carbon and nitrogen cycle that can be compared to ''reality'' are limited. Nitrogen source terms are summarized in Table 2, some other parameters in Table 3. Reality for NPP is largely what other models obtain, and the present model appears to be within that envelope. Table 4 compares simulated NPP with ranges as determined from those quoted in Bonan (1995). Agriculture appears to be high, possibly so biased from the constant addition of fertilizer and constant rate of harvest removal. The large NPP values for modeled tundra and needleleaf systems may indicate an inadequate treatment of cold temperature mortality.

The above-ground productivity of leaves, and in boles for woody plants, is well characterized for many systems. Where there is seasonal leaf drop, prescribing the leaf specific weights and modeling realistic LAIs is sufficient to give realistic leaf productivity. For evergreen leaves, given realistic LAI and leaf mass, the average leaf turnover rate is the main source of uncertainty. Because of its wide variation between species (Reich et al. 1992), it is difficult to infer an appropriate average value for a given system.

The parameterization of root turnover rate is problematical. Eissenstat and Yanai (1997) review factors believed to determine root turnover rates. One such factor is soil temperature. They suggest roots in colder soils should live longer in order to maximize the nutrient uptake per carbon cost over the lifetime of the roots. Older, less efficient roots, can be retained in cold soil because of low maintenance respiration costs. A recent global analysis of root turnover estimates that the Q10 of fine-root turnover is 1.4 for forests and 1.6 for grasslands (Gill and Jackson 2000). Steele et al., (1997) show for the BOREAS northern and southern sites, that daily root turnover decreased in the winter to only 10%–30% of summer rates. Hence, the model has assumed a root turnover dependence on temperature proportional to the square root of the respiration dependence, Eq. (7). Table 5 compares model fine-root masses with those summarized by Jackson et al. (1997). The root mass of the temperate grassland differs most with that observed. Since NPP of temperate grassland appears reasonable, agreement would only be possible with a large decrease in the rate of root turnover. If the tundra NPP were closer to the range of expected values, tundra root mass would be too low. It may be difficult to characterize root masses of Arctic ecosystems, as they are highly heterogeneous in their carbon storage characteristics (e.g., Shaver and Chapin 1991). The tropical forest root mass is nearly double that observed. The modeled NPP for roots in tundra and tropical broadleaf evergreen systems are 0.5 and 1.2 g m^{-2} day^{-1}, respectively, consistent with the factor of two difference in their computed root masses.

Table 6 shows the average content of different N reservoirs. The organic pool is low compared to observations because it does not include ''slow pools,'' that is, that locked up in humus, etc., and the plant pools do not include anything but that in leaves or roots, where agreement with observations is insured to the extent that we fit observed biomasses, since the observed N/C is built into the model. Hence, only the last two columns have neither built in disagreement or agreement and so would benefit most from observational comparisons.

Table 7 shows the external sources and sinks for N over the last year of simulation. All the rows are plausibly close to a balance except for the boreal (needleleaf evergreen) and tundra systems. For these, the annual deposition and smaller increment of natural fixation continues to largely be absorbed, mostly by the soil. Nitrification occurs at the same rates as elsewhere, but plant uptake and immobilization limits the nitrate to

TABLE 3. Other important parameters.

	Symbol	Value
Root N to C ratio (max)	r_{ncr}	0.024
Leaf structural N to C ratio (max)	r_{ncl}	0.03
CO_2 ppmv		360
Minimum LAI		0.1
Fraction of leaf of N not retranslocated	γ_r	0.5
Characteristic root mass	C_{ro}	250 g m^{-2}
Characteristic transpiration	ET_0	1.5×10^{-4} mm s^{-1}

TABLE 4. Model NPP g C m^{-2} day^{-1} compared to the range of values quoted by Bonan (1995).

Ecosystem	Current model	Bonan range
Crop/mixed farming	1.4	0.7–1.2
Grassland (short)	0.7	0.4–0.8
Evergreen needleleaf	1.2	0.6–1.4
Deciduous needleleaf	1.3	0.4–0.7
Deciduous broadleaf	2.1	1.1–2.1
Evergreen broadleaf	2.6	2.5–3.3
Shrub	0.7	0.3–1.2
Tundra	0.5	0.2–0.4

TABLE 5. Model live fine root mass kg C m^{-2} vs observations (Jackson et al. 1997).

Ecosystem	Observed	Model
Boreal	0.11	0.16
Temperate deciduous	0.22	0.23
Temperate grassland	0.42	0.14
Tropical grassland	0.25	0.35
Tropical evergreen	0.16	0.29
Tundra	0.16	0.16

TABLE 6. Model N reservoirs g m^{-2}.

System	Plant	Soil organic	Ammonium	Nitrate
Tundra	10	80	0.5	0.0
Needleleaf evergreen	15	100	1.2	0.1
Grassland	7	23	1.3	1.0
Cropland	5	38	1.7	1.2
Broadleaf evergreen	16	45	1.7	0.8
Global land	6.5	38	1.1	0.7

small values (e.g., Stark and Hart 1997). Both systems need an increase in their nitrate by a factor of 5 to be near balance. The observed low values of nitrate in high-latitude soils and rivers means either that we have greatly overestimated their supply of nitrogen or that they are always net sinks for N outside of catastrophic disturbances such as forest fires. The recent survey (Cleveland et al. 1999) of observed values for biological fixation indicates our modeled boreal forest values are on the high side, but tundra is on the low side. The Table 7 grassland fixation values are also on the high side of that observed.

5. Conclusions

Climate model parameterizations of land surface processes include stomatal controls on evapotranspiration. These controls in turn depend on canopy carbon uptake as driven by photosynthetic energy and leaf enzymes. This paper advances previous treatments of the stomatal controls by developing parameterizations for the following:

1) canopy Rubisco nitrogen for determining photosynthetic capacity;
2) allocation of the leaf structure, root, and labile plant nitrogen stores;
3) root and leaf respiration, the latter being supplied in part by photosynthetic energy during daytime;
4) instantaneous carbon allocation to leaves versus other plant reservoirs including a labile photosynthate store that supplies respiration requirements;
5) dependence on leaf-specific area (leaf area per leaf mass) of leaf structural nitrogen, leaf turnover, leaf lifetimes, and leaf internal resistance to carbon transport;
6) root nutrient uptake that balances physical transports by ET and diffusion, depending on soil water and root mass, with high- and low-affinity ion uptakes, the latter being reduced by negative feedbacks under conditions of canopy light limitation (or equivalently too much nitrogen).

Also developed are simple representations of other components of plant/soil nitrogen cycling individually similar to (but largely oversimplified relative to) treatments in other current biogeochemical-cycling models. Although subject to further improvement, together they significantly advance the coupling of the climate and biogeochemical systems, and include

1) soil organic stores supplied by death of plant carbon stores and corresponding plant nitrogen, and mineralized with carbon decomposition but with a fraction immobilized depending on soil–nitrogen ratio;
2) nitrification and denitrification depending on soil water and temperature;
3) leaching of nitrate by runoff;
4) biological fixation depending on temperature and on energy from plant photosynthate, and ceasing during periods of plant nutrient stress.

The parameterizations developed here include several feedbacks that limit Rubisco nitrogen amounts and hence dynamically force to some extent optimization between canopy photosynthetic capacities and levels of visible light including:

1) active ion uptake by roots is reduced at times when canopy photosynthesis is light limited;
2) photosynthate carbon is lost by Rubisco enzyme respiration, and in the absence of this photosynthate, the continuing leaf respiration is fueled by enzyme loss;
3) soil mineral nitrogen not taken up by roots is eventually lost by denitrification and leaching.

Overall, the parameterizations developed here are simple, require a limited number of parameters, and are hence easily coupled to existing canopy parameterizations in climate models. This coupling has been demonstrated for a 17-yr integration of a GCM climate model, forced by prescribed interannually varying sea surface temperatures. The conclusions from this simulation are the following:

TABLE 7. N source and sinks (g m^{-2} yr^{-1}).

System	Biological fixation	Deposition	Fertilization	Denitrification	Runoff
Tundra	0.1	0.5	0	0.1	0.0
Needleleaf evergreen	0.7	0.5	0	0.1	0.1
Grassland	1.5	0.5	0	1.3	0.4
Cropland	1.4	0.5	8.0	1.0	0.3
Broadleaf evergreen	2.8	0.5	0.0	2.0	1.0
Global land*	1.1	0.5	0.7	0.8	0.3

* Imbalance mostly from harvest removal.

1) the Rubisco canopy nitrogen and other nitrogen stores respond to interannual variations in climate variables such as precipitation and temperature;
2) these variations are manifested both by variations in LAI and root biomass and in leaf-level nitrogen;
3) hence, new mechanisms are included for climate feedback on the stomatal controls of evapotranspiration;
4) soil organic nitrogen in high latitude responds on decadal timescales to sources by storing nitrogen rather than by balancing with denitrification and leaching—catastrophic events such as fires may initiate most system loss of nitrogen;
5) NPP for individual biomes is in reasonable agreement with that of other models;
6) root biomass is reasonably consistent with observed values, except for modeled values for temperate grassland being too low and values for tropical forests being too high;
7) reasonable global budgets are obtained for the various nitrogen pools;
8) monthly averages over model grid points representing the Amazon forest and lower Colorado basin illustrate the coupled interannual variations of the evapotranspiration, LAI, Rubisco nitrogen, and NPP.

Acknowledgments. Support is acknowledged from NASA, through its IDS Program Grant (429-81-22;428-81-22) to the lead authors, and the Sellers, Mooney, Randall, Fung IDS at GSFC; G. B. Bonan's contribution was supported under the NSF funding of NCAR; W. A. Hoffmann and R. B. Jackson acknowledge support from NSF, NIGEC/DOE, and the Andrew Mellon Foundation.

APPENDIX

Some Symbols Used in Paper

b	Maximum carbon assimilation per g of Rubisco-related N
(T)	Enzymatic temperature dependence, Eq. (7)
f_n	Fraction of leaf structural and root nitrogen transferred to Rubisco pool
$f_{\rm cl}$	Fraction of carbon assimilated by leaves that is allocated either to leaf structure or photosynthate reservoirs
f_p	Fraction of carbon assimilated that is allocated to the photosynthate reservoir
$r_{\rm ncl}$	Ratio of nitrogen to carbon parameter for leaf structure
$r_{\rm ncr}$	Ratio of nitrogen to carbon parameter for roots
h_p	Light-limitation reduction of root physiological uptake, Eq. (22b)
$k_{\rm dn}$	Denitrification rate per unit NO_3^-, Eq. (29)
$k_{\rm lt}$	Leaf turnover rate, Eq. (18b)
k_m	Mineral nitrogen uptake rate per unit nitrogen, Eqs. (21)–(22)
$k_{\rm ni}$	Nitrification rate per unit NH_4^+, Eq. (28)
k_v	Ammonia volitization rate per unit NH_4^+
$k_{\rm ro}$	Runoff removal rate per unit NO_3^-, Eq. (30)
k_s	Scaling rate for cold and drought stress
r_r	Root radius = 0.5 mm
s	Soil moisture divided by saturated value
t	Time
w_c	Rubisco-limited rate, Eq. (8)
w_e	Export-limited rate, Eq. (10)
w_j	Light-limited rate, Eqs. (5)–(6)
A_n	Net carbon assimilated into leaf during daytime
C_l	Leaf carbon reservoir
C_r	Root carbon reservoir
C_p	Photosynthate carbon reservoir
C_s	Soil carbon reservoirs
$I_{\rm mob}$	Immobilization factor reducing rate of mineralization
F	Factor reducing rate of transfer of photosynthate to leaves from its maximum value
L_c	Specific leaf area (leaf area per unit leaf carbon)
LAI	Leaf area index over vegetated fraction of model grid square
N_l	Canopy total nitrogen pool
$N_{\rm ls}$	Canopy structural nitrogen pool
N_r	Root nitrogen
N_m	Soil mineral nitrogen = $NO_3^- + NH_4^+$
N_p	Total plant nitrogen store
$N_{\rm rub}$	Canopy Rubisco-related nitrogen pool
$\hat{N}_{\rm rub}$	Rubisco nitrogen per unit leaf area, either as a function of LAI or as a canopy average
N_s	Soil organic nitrogen store
R_d	Daytime canopy leaf respiration
R_n	Nightime canopy leaf respiration
R_r	Rubisco-related leaf respiration, Eq. (17)
$S_{\rm cd}$	Sum of cold and drought stress factors defined in Dickinson et al. (1998)
S_r	Fraction of leaf allocation not moved to roots under nitrogen stress
S_n	Fraction of allocation otherwise going to leaf that is diverted to roots because of nitrogen stress
T	Canopy temperature
X_c	Leaf carbon assimilation per unit time
V_m	Maximum leaf rate of carbon assimilation at a given temperature, Eq. (9)
γ_r	Fraction of leaf nitrogen returned to soil organic pool upon leaf death
λ_c	Computed ratio of CO_2 outside leaf to that at Rubisco site
λ_d	Maximum diffusion rate of root uptake per unit N_m
$\lambda_{\rm et}$	Maximum ET rate of root uptake per unit N_m
λ_r	Rate of ion affinity maximum root uptake per unit N_m
λ_t	Maximum transport rate of root uptake per unit $N_m = \lambda_d + \lambda_{\rm et}$
σ_f	Fraction of GCM grid square covered by vegetation

REFERENCES

Aber, J. D., S. V. Ollinger, and C. T. Driscoll, 1997: Modeling nitrogen saturation in forest ecosystems in response to land use and atmospheric deposition. *Ecol. Modell.,* **101,** 61–78.

Amthor, J. S., 1994: Scaling CO_2 photosynthesis relationships from the leaf to the canopy. *Photosynth. Res.,* **39,** 321–350.

Barber, S. A., 1984: *Soil Nutrient Bioavailability: A Mechanistic Approach.* John Wiley and Sons, 398 pp.

Bonan, G. B., 1995: Land–atmosphere CO_2 exchange simulated by a land surface process model coupled to an atmospheric general circulation model. *J. Geophys. Res.,* **100,** 2817–2831.

Bouwman, A. F., D. S. Lee, W. A. Asman, F. J. Dentener, K. W. Van Der Hoek, and J. G. J. Olivier, 1997: A global high-resolution emission inventory for ammonia. *Global Biogeochem. Cycles,* **11,** 561–587.

Chapin, F. S., 1991: Integrated responses of plants to stress: A centralized system of physiological responses. *Biosciences,* **41,** 29–35.

Cleveland, C. C., and Coauthors, 1999: Global patterns of terrestrial biological nitrogen (N_2) fixation in natural ecosystems. *Global Biogeochem. Cycles,* **13,** 632–646.

Collatz, G. J., J. T. Ball, C. Grivet, and J. A. Berry, 1991: Physiological and environmental regulation of stomatal conductance, photosynthesis and transpiration: A model that includes a laminar boundary layer. *Agric. For. Meteor.,* **54,** 107–136.

Dang, Q.-L., H. A. Margolis, M. Sy, M. R. Coyea, G. J. Collatz, and C. L. Walthall, 1997: Profiles of photosynthetically active radiation, nitrogen and photosynthetic capacity in the boreal forest: Implications for scaling from leaf to canopy. *J. Geophys. Res.,* **102,** 28 845–28 859.

Davidson, E. A., and J. L. Hackler, 1994: Soil heterogeneity can mask the effects of ammonium availability on nitrification. *Soil Biol. Biochem.,* **26,** 1449–1453.

Dentener, F. J., and P. J. Crutzen, 1994: A three-dimensional model of the global ammonia cycle. *J. Atmos. Chem.,* **19,** 331–369.

Dewar, R. D., B. E. Medlyn, and R. E. McMurtrie, 1998: A mechanistic analysis of light and carbon use efficiencies. *Plant, Cell Environ.,* **21,** 573–588.

Dickinson, R. E., A. Henderson-Sellers, and P. J. Kennedy, 1993: Biosphere–Atmosphere Transfer Scheme (BATS) for the NCAR Community Climate Model. NCAR Tech. Note NCAR/TN-387 + STR, 78 pp.

——, M. Shaikh, R. Bryant, and L. Graumlich, 1998: Interactive canopies for a climate model. *J. Climate,* **11,** 2823–2836.

Eissenstat, D. M., and R. D. Yanai, 1997: The ecology of root lifespan. *Advances in Ecological Research,* M. Begon and A. H. Fitter, Eds., Vol. 27, Academic Press, 1–59.

Esquível, M. G., R. B. Ferreira, and A. R. Teixeira, 1998: Protein degradation in C_3 and C_4 plants with particular reference to ribulose bisphosphate carboxylase and glycolate oxidase. *J. Exp. Bot.,* **49,** 807–816.

Evans, J. R., and S. von Caemmerer, 1996: Carbon dioxide diffusion inside leaves. *Plant Physiol.,* **110,** 339–346.

Farquhar, G. D., S. von Caemmerer, and J. A. Berry, 1980: A biochemical model of photosynthetic CO_2 assimilation in leaves of C_3 species. *Planta,* **149,** 78–90.

Field, C., 1983: Allocating leaf nitrogen for the maximization of carbon gain: Leaf age as a control on the allocation program. *Oecologia,* **56,** 341–347.

——, and H. A. Mooney, 1986: The photosynthesis-nitrogen relationship in wild plants. *On the Economy and Form of Plant Function,* T. J. Givnish, Ed., Cambridge University Press, 25–55.

Foley, J. A., I. C. Prentice, N. Ramankutty, S. Levis, D. Pollard, S. Sitch, and A. Haxeltine, 1996: An integrated biosphere model of land surface processes, terrestrial carbon balance, and vegetation dynamics. *Global Biogeochem. Cycles,* **10,** 603–628.

Foyer, C. H., and J. Harbinson, 1997: The photosynthetic electron transport system: Efficiency and control. *A Molecular Approach to Primary Metabolism in Higher Plants,* C. H. Foyer and W. P. Quick, Eds., Taylor and Francis, 3–40.

Galloway, J. N., W. H. Schlesinger, H. Levy II, A. Michaels, and J. L. Schnoor, 1995: Nitrogen fixation: Anthropogenic enhancement-environmental response. *Global Biogeochem. Cycles,* **9,** 235–252.

Gill, R. A., and R. B. Jackson, 2000: Global patterns of root turnover for terrestrial ecosystems. *New Phytol.,* **147,** 13–31.

Gordon, W. S., and R. B. Jackson, 2000: Nutrient concentrations in fine roots. *Ecology,* **81,** 275–280.

Gutschick, V. P., 1981: Evolved strategies in nitrogen acquisition by plants. *Amer. Naturalist,* **5,** 607–637.

Haxeltine, A., and I. C. Prentice, 1996: A general model for the light-use efficiency of primary production. *Funct. Ecol.,* **10,** 551–561.

Holland, E. A., and Coauthors, 1997: Variations in the predicted spatial distribution of atmospheric nitrogen deposition and their impact on carbon uptake by terrestrial ecosystems. *J. Geophys. Res.,* **102,** 15 849–15 866.

Howarth, R. W., and Coauthors, 1996: Regional nitrogen budgets and riverine N & P fluxes for the drainages to the North Atlantic Ocean: Natural and human influences. *Biogeochemistry,* **35,** 75–139.

Jackson, R. B., H. A. Mooney, and E.-D. Schulze, 1997: A global budget for fine root biomass, surface area, and nutrient contents. *Proc. Nat. Acad. Sci. U. S. A.,* **94,** 7362–7366.

Jungk, A., and N. Claassen, 1997: Ion diffusion in the soil–root system. *Adv. Agron.,* **61,** 53–110.

Kiehl, J. T., J. J. Hack, G. B. Bonan, B. A. Boville, D. L. Williamson, and P. J. Rasch, 1998: The National Center for Atmospheric Research Community Climate Model: CCM3. *J. Climate,* **11,** 1131–1149.

Kronzucker, H. J., M. Y. Siddiqi, and A. D. M. Glass, 1996: Kinetics of NH_4^+ influx in spruce. *Plant Physiol.,* **110,** 773–779.

Li, C., S. Frolking, and T. A. Frolking, 1992: A model of nitrous oxide evolution from soil driven by rainfall events. Part I: Model structure and sensitivity. *J. Geophys. Res.,* **97,** 9777–9796.

Long, S. P., W. F. Postl, and H. R. Bolhar-Nordenkampf, 1993: Quantum yields for uptake of carbon dioxide in C3 vascular plants of contrasting habitats and taxonomic groupings. *Planta,* **189,** 226–234.

Matthews, E., 1994: Nitrogen fertilizers: Global distribution of consumption and associated emissions of nitrous oxide and ammonia. *Global Biogeochem. Cycles,* **8,** 411–439.

McNaughton, S. J., N. R. H. Stronach, and N. J. Georgiadis, 1998: Combustion in natural fires and global emissions budgets. *Ecol. Appl.,* **8,** 464–468.

Moorhead, D. L., W. S. Currie, E. B. Rastetter, W. J. Parton, and M. E. Harmon, 1999: Climate and litter quality controls on decomposition: An analysis of modeling approaches. *Global Biogeochem. Cycles,* **13,** 575–590.

Ourry, A., A. J. Gordon, and J. H. Macduff, 1997: Nitrogen uptake and assimilation in roots and root modules. *A Molecular Approach to Primary Metabolism in Higher Plants,* C. H. Foyer and W. P. Quick, Eds., Taylor and Francis, 237–254.

Parton, W. J., A. R. Mosier, D. S. Ojima, D. W. Valentine, D. S. Schimel, K. Weier, and A. E. Kulmala, 1996: Generalized model for N_2 and N_2O production from nitrification and denitrification. *Global Biogeochem. Cycles,* **10,** 401–412.

Poorter, H., and J. R. Evans, 1998: Photosynthetic nitrogen-use efficiency of species that differ inherently in specific leaf area. *Oecologia,* **116,** 26–33.

Potter, C. S., P. A. Matson, P. M. Vitousek, and E. A. Davidson, 1996: Process modeling of controls on nitrogen trace gas emissions from soils worldwide. *J. Geophys. Res.,* **101,** 1361–1377.

Pregitzer, K. S., M. J. Laskowski, A. J. Burton, V. C. Lessard, and D. R. Zak, 1998: Variation in sugar maple root respiration with root diameter and depth. *Tree Physiol.,* **18,** 665–670.

Quick, W. P., and H. E. Neuhaus, 1997: The regulation and control of photosynthetic carbon assimilation. *A Molecular Approach*

to Primary Metabolism in Higher Plants, C. H. Foyer and W. P. Quick, Eds., Taylor and Francis, 41–62.

Reich, P. B., M. B. Walters, and D. S. Ellsworth, 1992: Leaf life-span in relation to leaf, plant and stand processes in diverse ecosystems. *Ecol. Monogr.,* **62,** 365–392.

——, B. D. Kloeppel, D. S. Ellsworth, and M. B. Walters, 1995: Different photosynthesis-nitrogen relations in deciduous hardwood and evergreen coniferous tree species. *Oecologia,* **104,** 24–30.

——, M. B. Walters, D. S. Ellsworth, J. M. Vose, J. C. Volin, C. Gresham, and W. D. Bowman, 1998: Relationships of leaf dark respiration to leaf nitrogen, specific leaf area and leaf life-span: A test across biomes and functional groups. *Oecologia,* **114,** 471–482.

Sanhueza, E., and P. J. Crutzen, 1998: Budgets of fixed nitrogen in the Orinoco Savannah region: Role of pyrodenitrification. *Global Biogeochem. Cycles.,* **12,** 653–666.

Seligman, N. G., R. S. Loomis, J. Burke, and A. Abshahi, 1983: Nitrogen nutrition and phenological development in field-grown wheat. *J. Agric. Sci.,* **101,** 691–697.

Sellers, P. J., J. A. Berry, G. J. Collatz, C. B. Field, and F. G. Hall, 1992: Canopy reflectance, photosynthesis and transpiration. Part III: A reanalysis using enzyme kinetics-electron transport models of leaf physiology. *Remote Sens. Environ.,* **42,** 187–216.

——, and Coauthors, 1996: A revised land surface parameterization (SiB2) for atmospheric GCMs. Part II: The generation of global fields of terrestrial biophysical parameters from satellite data. *J. Climate,* **9,** 676–705.

——, and Coauthors, 1997: Modeling the exchange of energy, water and carbon between continents and the atmosphere. *Science,* **275,** 502–509.

Serraj, R., T. R. Sinclair, and L. C. Purcell, 1999: Symbiotic N_2 fixation response to drought. *J. Exp. Bot.,* **50,** 143–155.

Shaver, G. R., and F. S. Chapin III, 1991: Production: Biomass relationships and element cycling in contrasting Arctic vegetation types. *Ecol. Monogr.,* **61,** 1–31.

Smith, K. A., 1997: The potential for feedback effects induced by global warming on emissions of nitrous oxide by soils. *Global Change Biol.,* **3,** 327–338.

Stark, J. M., and S. C. Hart, 1997: High rates of nitrification and nitrate turnover in undisturbed coniferous forests. *Nature,* **385,** 61–64.

Steele, S. J., S. T. Gower, J. G. Vogel, and J. M. Norman, 1997: Root mass, net primary production and turnover in aspen, jack pine and black spruce forests in Saskatchewan and Manitoba, Canada. *Tree Physiol.,* **17,** 577–587.

Vinther, F. P., 1998: Biological nitrogen fixation in grass-clover affected by animal excreta. *Plant Soil,* **203,** 207–215.

Wullschleger, S. T., 1993: Biochemical Limitations to Carbon Assimilation in C_3 Plants—A retrospective analysis of the A/C_j curves from 109 species. *J. Exp. Bot.,* **44,** 907–920.